Scattering map for two black holes

Alessandro P. S. de Moura*

Instituto de Fíisca Gleb Wataghin, UNICAMP, 13083-970 Campinas, SP, Brazil

Patricio S. Letelier†

*Instituto de Matemática, Estatística e Ciência da Computação, Departamento de Matemática Aplicada, UNICAMP,
13083-9790 Campinas, SP, Brazil*

We study the motion of light in the gravitational field of two Schwarzschild black holes, making the approximation that they are far apart, so that the motion of light rays in the neighborhood of one black hole can be considered to be the result of the action of each black hole separately. Using this approximation, the dynamics is reduced to a two-dimensional map, which we study both numerically and analytically. The map is found to be chaotic, with a fractal basin boundary separating the possible outcomes of the orbits (escape or falling into one of the black holes). In the limit of large separation distances, the basin boundary becomes a self-similar Cantor set, and we find that the box-counting dimension decays slowly with the separation distance, following a logarithmic decay law.

PACS number(s): 05.45.Df, 95.10.Fh, 04.70.Bw

I. INTRODUCTION

In this paper we study the motion of light (null geodesics) in the gravitational field of two nonrotating Schwarzschild black holes. In general relativity, solutions of the field equations describing more than one purely gravitational source are necessarily nonstationary because gravity is always attractive (we are not considering exotic matter); there is no possibility of arbitrarily ''pinning'' sources as is done in Newtonian gravitation, because of the automatic self-consistency of the nonlinear Einstein's equations. If we demand that the two black holes be fixed in space, then the solution includes a conical singularity (a ''strut'') lying on the axis on which the two masses are located [1]. This singularity appears as a natural consequence of the field equations, and it is necessary to keep the two masses from falling towards each other. However, this singularity would have to be made of very exotic matter, and this solution does not describe any realistic system in astrophysics. The real solution to the relativistic two-body problem can have no conical singularities, and it is necessarily nonstationary. The two black holes will spiral around each other, emitting gravitational waves, which makes this problem even more difficult. There is no exact solution for the relativistic two-body problem, and even a numerical solution has eluded the most powerful computers.

In order to cope with this problem, Contopoulos [2] and Dettman *et al.* [3] have used the Majumdar-Papapetrou solution [1] to study the dynamics of test particles in a space-time with two black holes (test particles are particles with negligible mass and no internal degrees of freedom). The Majumdar-Papapetrou metric used by Contopoulos describes

two nonrotating black holes with extreme electric charge ($Q=M$ in relativistic units), whose gravitational pull is exactly matched by their electrostatic repulsion, thereby allowing a static mass configuration. They have found that in this metric the motion of both light and massive particles is chaotic, with a fractal invariant set and a fractal basin boundary. However, it is very unlikely that the Majumdar-Papapetrou metric describes realistic astronomical objects, since there is no known realistic astrophysical process by which a black hole with extreme charge could be formed. Even though the two black holes with extreme charge have proven to be a useful model, it is interesting to address the problem of two uncharged black holes, even if using an idealized model. This is what we do in this paper, for the motion of light and other massless particles. Our model is admittedly highly idealized, but nevertheless we think it keeps some of the basic features of the dynamics of the real system, besides being an interesting dynamical system by itself.

In order to overcome the fact that there is no static solution for the two-black-hole system, we consider the case when the two black holes are far apart, with a distance much larger than their Schwarzschild radii. In this case, nonlinear effects in the field equations are expected to be small, and we can approximate the motion of test particles in the neighborhood of one of the masses as being the result of the field of that mass alone and disregard the effect of the other black hole as being negligible. Using this approximation, the motion of test particles in the two-black-hole system is treated as a combination of motions caused by isolated Schwarzschild black holes. Since the equations of motion for the Schwarzschild geometry can be analytically integrated, our dynamical system is reduced to a map, which is much easier to study than a system of ordinary differential equations. This scattering map is built in Sec. II for the simple case of two black holes with equal masses. In Sec. III we show that this map has a fractal basin boundary separating the possible outcomes of a light ray in the two-black-hole field, namely, falling into either of the black holes or escaping towards the

---

*Present address: College of Computer, Mathematical and Physical Sciences, University of Maryland, College Park, MD 20742-3511. Email address: amoura@glue.umd.edu

†Email address: letelier@ime.unicamp.br

asymptotically plane infinity. The fractal (box-counting) dimension of this basin boundary is numerically calculated, and the sensitivity to initial conditions implied by the fractal nature of the boundary is thereby quantified. In Sec. IV we use explicitly the condition of large separation between the black holes. In this limit, the basin boundary becomes a self-similar Cantor set, which allows us to obtain analytical results on the fractal dimension of the basin boundary and its dependence on the distance between the black holes. We find that the fractal dimension decays very slowly (logarithmically) with distance. In Sec. V, we consider the case of two black holes with unequal masses, in the limit of a large separation; we find that the logarithmic decay law of the fractal dimension for large distances is also valid in this case. In Sec. VI, we summarize our results and draw some conclusions.

II. SCATTERING MAP FOR TWO BLACK HOLES WITH EQUAL MASSES

We begin by reviewing some basic results concerning the motion of test particles in the field of an isolated Schwarzschild black hole [4,5]. We consider specifically the case of null geodesics (trajectories of particles with zero rest mass, such as photons), which concerns us most, but many features of the dynamics also apply to massive particles.

The Schwarzschild metric is written in spherical coordinates as

$$ds^2 = \left(1 - \frac{2M}{r}\right) dt^2 - \frac{dr^2}{1 - \frac{2M}{r}} - r^2 d\Omega^2,$$

with $d\Omega^2 = d\theta^2 + \sin^2\theta d\phi^2$ being the element of area on a unit sphere, and t is the time measured from a distant observer. M is the black hole's mass in geometrized units ($G = c = 1$). We are interested only in the region of space-time outside the event horizon, $r > 2M$. Due to the conservation of angular momentum, test particles move on a plane, which can be chosen as $\theta = \pi/2$. The plane whereon the motion occurs is then described by the coordinates r and ϕ. The geodesic equations that describe trajectories of test particles on this plane can be analytically integrated by means of elliptical functions [4]. Here we are interested in the scattering of null geodesics by the black hole. A light ray coming from infinity towards the black hole is characterized by the impact parameter b defined by the ratio $b = L/E$, where the angular momentum L and the energy E are constants of motion given by

$$E = \left(1 - \frac{2M}{r}\right) \frac{dt}{d\lambda},$$

$$L = r^2 \frac{d\phi}{d\lambda}.$$

λ is the geodesic's affine parameter. For null geodesics only the ratio of L and E is of importance to the dynamics. In the asymptotically plane region $r \rightarrow \infty$, b corresponds to the usual impact parameter of classical scattering problems.
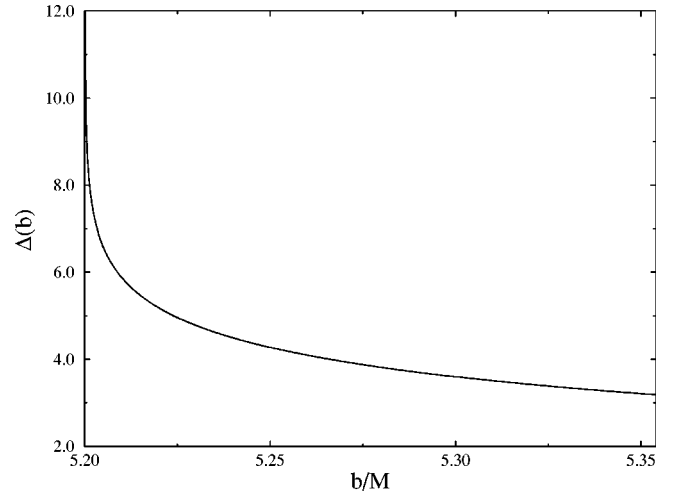

FIG. 1. The deflection function $\Delta(b)$ for an isolated Schwarzschild black hole.

If the impact parameter is below the critical value $b_c = 3\sqrt{3}M$, the trajectory of the light ray spirals down the event horizon and plunges into the black hole. If $b > b_c$, the trajectory circles the black hole and escapes again towards infinity, being deflected by an angle Δ. The lowest value P of the radial coordinate r along the trajectory (the ''perihelium'') is given by

$$b^2 = \frac{P^3}{P - 2M}. \tag{1}$$

Following Chandrasekhar [4], we define the quantities Q, k and χ by

$$Q^2 = (P - 2M)(P + 6M), \tag{2}$$

$$k^2 = \frac{Q - P + 6M}{2Q}, \tag{3}$$

$$\sin^2(\chi/2) = \frac{Q - P + 2M}{Q - P + 6M}. \tag{4}$$

The scattering angle Δ is then given by

$$\Delta = \pi - 2f(b), \tag{5}$$

and the function $f(b)$ is

$$f(b) = 2\sqrt{\frac{P}{Q}}[K(k) - F(\chi/2, k)]. \tag{6}$$

Here F is the Jacobian elliptic integral and K is the complete elliptic integral. In Fig. 1 we show a plot of $\Delta(b)$. As b approaches the critical value b_c from above, Δ goes to infinity; trajectories with b sufficiently near b_c can circle the black hole an arbitrary number of times before escaping, and for $b = b_c$, the light ray makes an infinite number of rotations, and never escapes. This is a consequence of the existence of an unstable periodic orbit at $r = 3M$, which appears as a maximum in the effective potential. The orbits with b

$=b_c$ spiral towards the $r=3M$ orbit, and in the language of dynamical systems they make up the stable manifold associated with this periodic orbit.

The fact that Δ assumes values above π for a nonzero range of b implies the existence of a rainbow singularity in the scattering cross section; this is to be contrasted with the Newtonian Rutherford scattering, which shows no such singularities. In fact, Δ assumes arbitrarily large values, and the differential cross section at any given angle θ is made up of an infinite number of contributions arising from trajectories with $\Delta=\theta$, $\Delta=\theta+2\pi$, in general, $\Delta=\theta+2n\pi$, corresponding to trajectories that circle the black hole n times before being scattered towards θ. However, large values of n correspond to very low ranges of b: the set of trajectories that scatters by $\theta+2n\pi$ has a measure that decreases very rapidly with n. Chandrasekhar [4] shows that the impact parameter b_n corresponding to a scattering by $\theta+2n\pi$ for large values of n is given approximately by

$$b_n=b_c+3.48Me^{-(\theta+2n\pi)}. \tag{7}$$

This expression shows that the measure of the set of trajectories scattered by $\theta+2n\pi$ decays exponentially with n, and the contribution of orbits with large n to the cross section is small. In fact, we shall see later that in many cases it is a good approximation to consider only orbits with $n=0$.

After reviewing some properties of an isolated black hole, we now consider the case of two black holes with equal mass M (we consider the case of different masses in Sec. V). As we mentioned in the Introduction, there is no exact solution of Einstein's field equations that describes this system. Because of this, we assume that the two black holes are separated by a distance D much larger than their Schwarzschild radius $2M$; in this limit the nonlinear interaction between the two gravitational fields can be ignored. In a real system, the two black holes will be rotating around their center of mass; however, their rotation speed is much smaller than the velocity of light. We can thus consider the two black holes to be fixed in space, without incurring in too much error (this approximation is further justified in the end of this Section). Notice that this approximation might not be valid for massive test particles (except in the ultrarelativistic limit, when when the trajectories are well approximated by null geodesics). Even though our approximations are admittedly crude, we believe they still retain some relationship with the real system.

We are interested in the orbits that never escape to infinity or fall into one of the event horizons; these orbits make up the basin boundary of the system, which will be discussed later in more detail. For the orbits not to escape, they need to have impact parameters such that they are scattered by at least π by one of the black holes. In the case of an isolated black hole, this corresponds to an impact parameter lower than $b=b_{esc}\approx 5.356\,96M$, which is less than three times the Schwarzschild radius. Since in our approximation $D\gg 2M$, for the purpose of finding the basin boundary we can consider that the light rays are scattered by each black hole separately, the other black hole being too far away to make a significant difference in the scattering. After suffering a scattering by one of the black holes, the ray may reach the other black hole, depending on its emerging trajectory after the
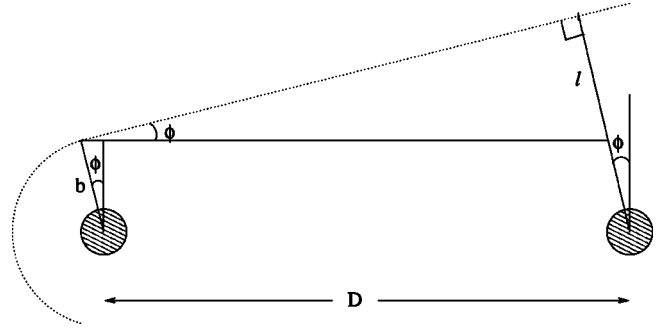

FIG. 2. Construction of the scattering map. The dotted line represents the trajectory of a light ray.

first scattering. It is then scattered again, and may return to the first black hole, and so on. Since $D\gg 2M$, we consider the scattering process of each black hole separately and use formulas (5) and (6) to determine the deflection angle due to each black hole as a function of the incident impact parameter.

By making the approximations mentioned above, we reduce the motion of light in the two-black-hole space-time to a two-dimensional (2D) map, as has been done in [6] (see also [7]) to study general features of chaotic scattering. To do this, we make the further assumption that the light rays have zero angular momentum in the direction of the axial symmetry axis, on which lie the two black holes; the orbits are then confined to a plane containing the two black holes. Due to the axial symmetry of the system, the motions on all such planes are similar. Now suppose we have a light ray escaping from one of the black holes with impact parameter b_n and with an escaping angle ϕ_n with respect to the symmetry axis, as shown schematically in Fig. 2. Since the black holes are considered to be very far apart, the impact parameter b_{n+1} of the light ray with respect to the other black hole is the segment l shown in Fig. 2 (one black hole can be considered to be "at infinity" as regards the other). We use the convention that positive values of b mean that the ray is directed to the right side of the black hole, and rays with negative b are directed to the left; notice that "right" and "left" are defined with respect to the black hole the light ray is inciding on, and therefore the orientation is reversed after each iteration of the map. From elementary geometry, we have $l=b_n+D\sin\phi$. The deflection angle is given by $\Delta(b_{n+1})$. The map is then written as

$$b_{n+1}=b_n+D\sin\phi_n, \tag{8}$$

$$\phi_{n+1}=\pi+\phi_n-\Delta(b_{n+1}) \mod 2\pi. \tag{9}$$

The angles ϕ_n are measured counterclockwisely with respect to each black hole; again the orientation is reversed after each iteration. The first term in Eq. (9) comes from the change in the angle's orientation.

Consider the initial conditions $b_0=b_{esc}$ and $\phi_0=0$. Since $\Delta(b_{esc})=\pi$, we see from the above equations that these values of b and ϕ are a fixed point of the map. It corresponds to the periodic orbit depicted in Fig. 3(a), which revolves around the black holes, making a U-turn at each black hole and then heading towards the other. Another periodic orbit is shown in Fig. 3(b). This orbit is such that $b_{n+1}=-b_n$ and
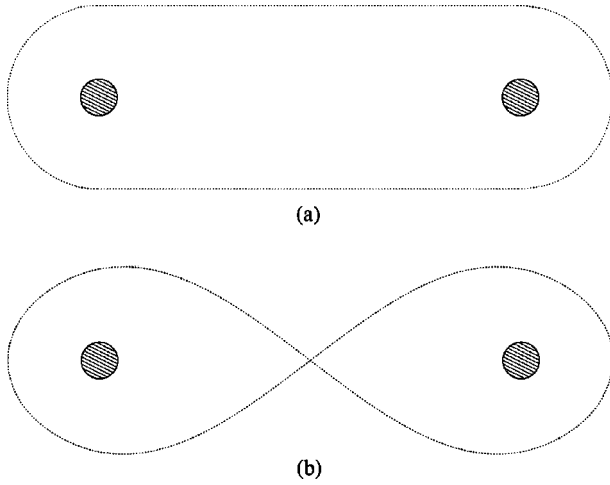
FIG. 3. Two examples of periodic orbits of the scattering map.

$\phi_{n+1} = -\phi_n$. Inserting these conditions in Eqs. (8) and (9), we find $2b_0 = -D \sin \phi_0$ and $\Delta(b_0) = \pi + 2|\phi_0|$ (remember that the angles are defined modulus 2π), with $b_0 > 0$. ϕ_0 is given by the solution of the equation

$$\Delta\left(\frac{D}{2}\sin|\phi_0|\right) = \pi + 2|\phi_0|.$$

These are the simplest periodic orbits, but there are many others.

We observe that Eqs. (8) and (9) are valid only as long as b remains within the range $b_c < b < b_{esc}$. If b falls out of this interval, the ray either escapes or falls into one of the black holes, and the iteration must be stopped.

We now analyze the validity of the approximations we made to obtain Eqs. (8) and (9). There are three approximations involved: (1) the assumption that the trajectories of light rays near one black hole are not significantly affected by the other black hole's gravitational field; (2) the assumption that the rotation of the black holes around the system's center of mass can be neglected; and (3) the exclusion of general relativistic effects such as the emission of gravitational waves.

To analyze the first approximation, consider a light ray with impact parameter b. Only light rays with b of the order of b_{esc} do not immediately escape to infinity, so these are the important ones for the dynamics. Their distance to the black hole (the near one) is of the order of b_{esc}, which is of the order of M. We can roughly estimate the gravitational field felt by these rays to be of the order of $M/b_{esc} \sim 1$. The gravitational field of the distant black hole, on the other hand, is of the order of M/D, and therefore the correction term to the gravitational field due to the presence of the distant black hole is $\sim M/D$, which vanishes as $D \to \infty$.

The rotation of the black holes around their common center of mass causes the axis defined by the center of the two black holes to rotate by an angle α in the time Δt it takes for a light ray to cross the distance D separating the two black holes. We have $\Delta t \approx D$. The rotation frequency ω can be approximated by Kepler's law: $\omega^2 \sim M/D^3$. α is thus given by

$$\alpha = \omega \Delta t \sim \left(\frac{M}{D}\right)^{1/2}. \quad (10)$$

Since $\alpha \to 0$ for large distances, the approximation is thus justified.

The general-relativistic corrections are more difficult to evaluate, but one can have some idea of the order of their magnitude by considering the rate of change $\dot{D}$ of the separation distance caused by the loss of energy by the system to the emission of gravitational waves. In [8] it is shown that $\dot{D}$ in the limit of large M/D is proportional to $(M/D)^3$. Defining ΔD to be the variation of D in the time it takes for a light ray to cross the distance between the black holes, we have

$$\frac{\Delta D}{D} \sim \left(\frac{M}{D}\right)^3. \quad (11)$$

Although the relativistic contributions to the motion of the particle is not restricted to the change of D, it is not unreasonable to expect that the other contributions have the same order of magnitude. In the case of black holes with two different masses, all the previous estimates remain valid, with M replaced by $\max(M_a, M_b)$, where M_a and M_b are the masses of the black holes.

III. ANALYSIS OF THE SCATTERING MAP

In this section we proceed to study in detail the map defined by Eqs (8) and (9). We begin by a direct numerical investigation of these equations (for a particular separation distance), which reveals a fractal structure in the boundary between the initial conditions corresponding to different escapes. We then proceed to explain how this fractal structure arises from the dynamics of the map [Eqs. (8) and (9)]. Finally, we use the large separation approximation to obtain some analytic results on the fractal dimension and other quantities related to the basin boundary.

A. Numerical investigation of the scattering map

In order to iterate Eqs (8) and (9) for given initial values ϕ_0 and b_0, we first have to be able to calculate the deflection angle Δ for a given impact parameter b. To do this, we must begin by finding the ''perihelium distance'' P corresponding to b; this is done by solving the third-order equation (1) for P. We use the well-known Newton-Raphson method, which guarantees a very fast convergence [9]. We then use Eqs. (2), (3), and (4) to calculate Q, k, and χ, and we finally substitute these quantities in Eqs. (5) and (6) to obtain $\Delta(b)$. The elliptical functions F and K are computed by numerical routines found in [9].

Depending on its initial conditions, a light ray may either fall into one black hole, fall into the other black hole, or escape towards infinity. The set of initial conditions which leads to each of these outcomes is called the *basin* of that outcome. In our numerical iteration of the map [Eqs. (8) and (9)], we are interested in obtaining a basin portrait of the system. To do this, we have to choose a set of initial conditions and iterate them to find out to which basin they belong. Our choice is the one-dimensional set with $\phi_0 = 0$ and an interval of b. As we have seen in Sec. II, if $|b| < b_c$, the light
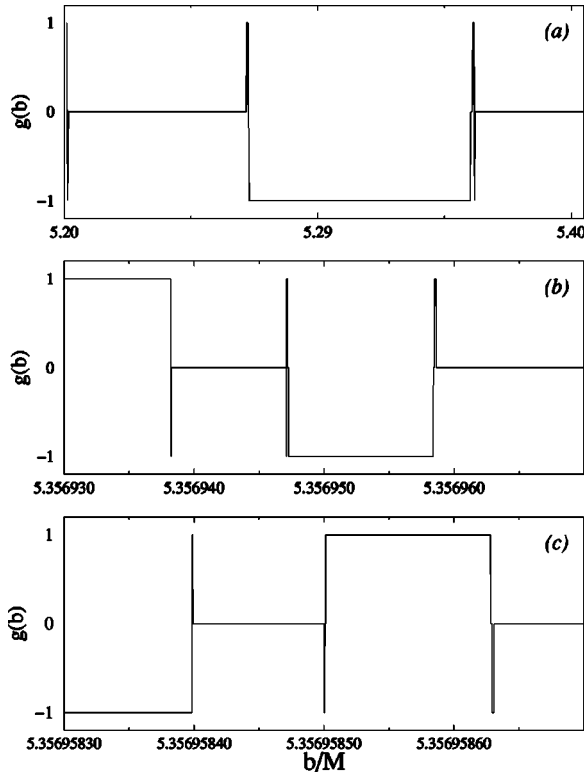
FIG. 4. Portrait of the basins as a function of the impact parameter b, for $\phi_0=0$. The ''basin function'' $g(b)$ is defined to be 1 if the orbit with initial conditions $\phi_0=0$, $b_0=b$ falls into one of the black holes, -1 if it falls into the other black hole, and 0 if it escapes to the asymptotically plane region. Even though the function $g(b)$ assumes only discrete values, the points are connected by straight lines for better visualization. Two successive magnifications of a small region of the initial interval are pictured, showing the fractal dependency of g on b.

ray always falls into the event horizon, and if $|b|>b_{esc}$, it always escapes. We thus choose the interval to be $b_c<b<b_{esc}$. We divide this segment into 5000 points, and iterate the map [(8) and (9)] for each of these initial conditions, recording the final outcome for each point: if at any point in the iteration $|b_n|<b_c$, this means that the light ray falls into one of the black holes, and if $|b_n|>b_{esc}$, it escapes to infinity. We define the discrete-valued function $g(b)$ to be 1 if the orbit with initial conditions $\phi_0=0$, $b_0=b$ falls into one of the black holes, -1 if it falls into the other, and 0 if it escapes to the asymptotically plane region. $g(b)$ gives a picture of the intersections of the three basins with the segment $\phi_0=0$, $b_c<b<b_{esc}$.

The result is shown in Fig. 4(a) for $D=15M$. We see that there are large intervals in which g is constant, intercalated by ranges of b where g varies wildly. If b_0 lies within one of these latter ranges, the final outcome of the light ray is highly uncertain. In Fig. 4(b) we show a magnification of one of these regions. Except for the scale, it is very similar to Fig. 4(a). A further magnification is shown in Fig. 4(c), again revealing structure in small scales. We have obtained even further magnifications, which are not shown here, and all show similar structures, down to the smallest scales allowed by the numerical limitations. This shows that g has a fractal dependence on b. Notice that there are large intervals of b where g is perfectly regular. These regular regions are mixed

in all scales with the fractal regions, where the outcome of a light ray is highly uncertain. This sensitivity of the dynamics to the initial conditions is made precise with the definition of the *box-counting dimension*, which we now present briefly [10].

We define the *basin boundary* of the system to be the set of points (initial conditions) such that all neighborhoods of these points have points belonging to at least two different basins, no matter how small that neighborhood is. The fractal nature of the basins shown in Fig. 4 results from a fractal basin boundary [10]. It is not difficult to see that a fractal basin boundary implies a fundamental uncertainty in the final outcome of an orbit. We now define the box-counting dimension of the basin boundary, which gives a measure of this uncertainty. Let b_0 be a randomly chosen impact parameter in the interval $[b_c,b_{esc}]$; we consider $\phi_0=0$ throughout for simplification. Let $f(\epsilon)$ be the probability that there is a point of the basin boundary lying within a distance ϵ from b_0. In the limit $\epsilon\to 0$, f generally scales with ϵ by a power law. We thus write

$$f(\epsilon)\propto\epsilon^{1-d}. \tag{12}$$

d is the box-counting dimension of the intersection of the basin boundary with the one-dimensional section of initial conditions given by $b\in[b_c,b_{esc}]$ and $\phi_0=0$. Clearly, we must have $0\leq d\leq 1$. If the basin boundary is regular, then $d=0$; fractal boundaries have $d>0$. f can be interpreted as a measure of the uncertainty as to which basin the point b belongs, for a given error ϵ in the initial condition, which is always present in a real situation. For a regular basin boundary, f decreases linearly with ϵ. If we have a fractal boundary, however, the power in Eq. (12) is less than 1, and f decreases much more slowly with ϵ, which makes the uncertainty in the outcome much higher than in the case of a regular boundary. Thus, d is a good measure of the sensitivity to the initial conditions that results from a fractal basin boundary, and since it is a topological invariant [10], it is a meaningful characterization of chaos in general relativity.

We calculate the box-counting dimension d numerically by using the method we now explain [10]. We pick a large number of initial conditions b randomly, and for each one of them we compute the map [Eqs. (8) and (9)], finding out its outcome and therefore to which basin it belongs. We then do the same thing to the two neighboring initial conditions $b+\epsilon$ and $b-\epsilon$, for a given (small) ϵ, for each b. If the three points do not belong to the same basin, b is labeled an ''uncertain'' initial condition. For a large number of initial conditions, we expect that the fraction of uncertain points for a given ϵ approximates $f(\epsilon)$. Calculating in this way f for several values of ϵ, we use Eq. (12) to obtain d from the inclination of the log-log plot of f versus ϵ. Applied to the two-black-hole map with $D=15M$, this method gives $d=0.17\pm0.02$. The error comes from the statistical uncertainty which results from the finite number of points used in the computation of f. In our calculation, the number of initial conditions was such that the number of ''uncertain points'' is always higher than 200.
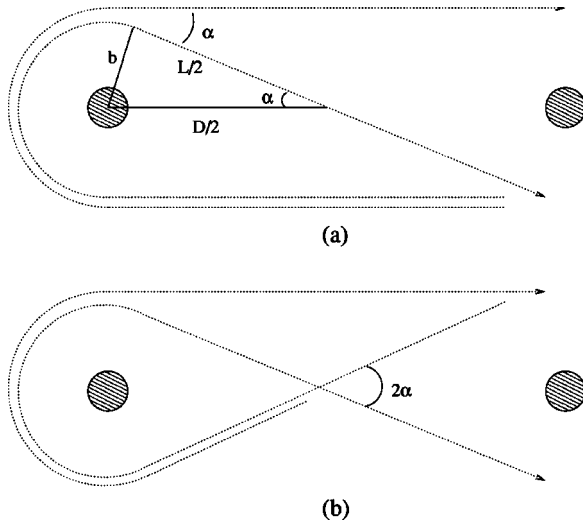
FIG. 5. (a) Two possible types of scatterings for an orbit which was previously scattered by $(2n+1)\pi$; (b) two scatterings for an orbit which was previously deflected by $(2n+1)\pi+\alpha$ or $(2n+1)\pi+2\alpha$.

B. The fractal basin boundary

How does the fractal basin boundary arise from the dynamics of the map [(8) and (9)]? In order to answer this question, we first observe that every point in the basin boundary gives rise to orbits that neither escape nor fall into one of the black holes (otherwise they would be part of one of the basins, which violates the definition of the basin boundary); that is, the basin boundary is made up of "eternal orbits" which move forever around the two black holes. We need thus to investigate these orbits to understand the formation of the basin boundary.

Consider the one-dimensional set of initial conditions parametrized by the impact parameter b with $\phi_0 = 0$. We have seen that if $|b| < b_c$ the orbit falls into the event horizon of a black hole, and if $|b| > b_{esc}$ the orbit escapes. Thus, the points of the basin boundary belong to the interval

$$|b| \in [b_c, b_{esc}], \qquad (13)$$

which is actually two disjoint intervals, corresponding to positive and negative values of b. However, not all points in this interval are part of the basin boundary, of course; in order to survive the next iteration of the map [(8) and (9)] without escaping or falling, the corresponding orbits must be deflected in such a way that they reach the other black hole with an impact parameter within the interval (13). From Fig. 5 we see that for this to happen the orbits must be deflected by an angle θ in the neighborhood of $(2n+1)\pi+\alpha$, and either $(2n+1)\pi$ or $(2n+1)\pi+2\alpha$, depending on the previous deflection suffered by the orbit; the angle α depends on the distance separating the black holes. n is the number of turns the orbit makes around one of the black holes before moving on to the other one. For each n, there are two intervals of the deflection angle θ for which the orbit survives the next iteration without escaping or falling; these two intervals correspond to the positive and negative values of b satisfying Eq. (13). In the first iteration, the initial interval (13) is divided into infinitely many pairs of subintervals, each pair labeled by the number n of times the orbit circles the black

hole. From Eq. (7), intervals corresponding to large n's decrease exponentially with n. In the next iteration, each of these subintervals is itself divided into an infinite number of intervals, and so on in the next iterations. This implies that the underlying symbolic dynamics of the system has an infinite alphabet (an infinite number of symbols). In the limit of infinite iterations, the set of surviving orbits is a fractal set with zero measure. This set is the basin boundary, and its fractality is responsible for the complex dynamics shown in Fig. 4. The two fractal regions on the right of Fig. 4(a) consist of orbits whose first scattering has $n=0$, that is, they are deflected by the black hole by π and $\pi+\alpha$. The leftmost fractal region in Fig. 4(a) is actually an infinite number of very small regions, corresponding to orbits with $n \neq 0$; the scale of Fig. 4(a) is too large for them to be distinguished. This gives us an indication that the orbits with $n>0$ are a very small fraction of the basin boundary; we shall return to this later in this section.

It is important to observe that the basin boundary is fractal because the scattering function $\Delta(b)$ of the isolated black hole (5) assumes values higher than π, which makes it possible for orbits to be scattered to both sides of the black hole, giving rise to the fractal basin boundary. The scattering of particles by two fixed Newtonian mass points is immediately seen to be regular, because Rutherford's scattering function does not assume values higher than π. This is of course in accordance with the fact that the fixed two-mass problem in Newtonian gravitation is integrable, since the Hamilton-Jacobi equation of this system is separated in elliptical coordinates [11].

C. Some analytical results

We have seen that after being scattered by a black hole, the light ray must have an impact parameter lying on the interval (13) to belong to the basin boundary. Since $b_c = 3\sqrt{3}M \approx 5.196\,15M$ and $b_{esc} \approx 5.356\,96M$, the impact parameter must belong to one of two intervals of length $\Delta b = b_{esc} - b_c \approx 0.160\,81M$ (the two intervals correspond to positive and negative impact parameters). In our approximation we have $\Delta b \ll D$. Using this fact, we can approximate the value of b in Fig. 5 by b_{esc}, with an error of Δb at worst, which means a fractional error of about $\Delta b / b_{esc} \approx 0.03$. The distance L in Fig. 5 traveled by orbits which were deflected by $(2n+1)\pi+\alpha$ or $(2n+1)\pi+2\alpha$ in the previous scattering is thus given by $(L/2)^2 + b_{esc}^2 = (D/2)^2$, that is,

$$L = \sqrt{D^2 - 4b_{esc}^2}. \qquad (14)$$

For the map [(8) and (9)] to be well defined, we must have $D > 2b_{esc}$. Of course, this condition is satisfied in our approximation $D \gg 2M$. The angle α is calculated from Fig. 5 in this approximation using elementary geometry

$$\sin \alpha = \frac{2b_{esc}}{D}. \qquad (15)$$

Consider a set of orbits with impact parameters filling the interval $[b_c, b_{esc}]$ of length Δb, which may have already suffered several previous scatterings. The subsets of these orbits that survive the next scattering without escaping nor

falling into one of the black holes are subintervals in the neighborhood of b_n^k, where b_n^k are the values of the impact parameter such that the orbit is deflected by an angle of $(2n+1)\pi + k\alpha$ ($k = 0$, 1, or 2). They are solutions of the algebraic equation

$$\Delta(b_n^k) = (2n+1)\pi + k\alpha, \qquad (16)$$

with Δ given by Eq. (5). The fractal regions of Fig. 4(a) are located around values of b given by Eq. (16) with $k = 0$ and $k = 1$. Depending on the previous deflections suffered by a given set of trajectories, the values $k = 1$ and $k = 2$ must be used instead in Eq. (16), according to the rules of the symbolic dynamics we exposed above.

Because the distance D is much larger than Δb, the allowed range in the deflection angle $\delta\theta_n^k$ around $(2n+1)\pi + k\alpha$ of an orbit such that it arrives at the other black hole with b in the interval (13) is approximately

$$\delta\theta_n^0 = \frac{\Delta b}{D}, \qquad \delta\theta_n^{1,2} = \frac{\Delta b}{L}, \qquad (17)$$

where L is given by Eq. (14). The length Δb_n^k of the interval of surviving orbits around b_n^k is in this approximation much smaller than Δb: $\Delta b_n^k \ll \Delta b$. We can therefore approximate Δb_n^k by the first-order expression $\Delta b_n^k \approx \delta\theta_n^k / |\Delta'(b_n^k)|$, with $\Delta' = d\Delta/db$. We define $\lambda_n^k = \Delta b_n^k / \Delta b$ as the fraction of the interval $[b_c, b_{esc}]$ (or $[-b_{esc}, -b_c]$) occupied by the surviving orbits with b around b_n^k. We have

$$\lambda_n^0 = \frac{1}{D|\Delta'(b_n^0)|}, \qquad \lambda_n^{1,2} = \frac{1}{L|\Delta'(b_n^{1,2})|}. \qquad (18)$$

Given a value of D, it is easy to solve Eq. (16) numerically for b_n^k, with L and α given by Eqs. (14) and (15). For $D = 15M$, we find $L \approx 10.5M$ and $\alpha \approx 0.7956$. By a direct numerical calculation of Δ and its first derivatives, we find

$$b_0^0 = b_{esc}, \quad \Delta'(b_0^0) = -5.863/M, \quad \Delta''(b_0^0) = 38.30/M^2,$$

$$b_0^1 = 5.266\,29M, \quad \Delta'(b_0^1) = -13.35/M,$$

$$\Delta''(b_0^1) = 202.5/M^2,$$

$$b_0^2 = 5.227\,29M, \quad \Delta'(b_0^2) = -31.66/M, \qquad (19)$$

$$\Delta''(b_0^2) = 1030/M^2,$$

$$b_1^0 = 5.196\,43M, \quad \Delta'(b_1^0) \approx -3600/M,$$

$$\Delta''(b_1^0) \approx 1.3 \times 10^7/M^2.$$

Here $\Delta'' = d^2\Delta/db^2$. The second derivative of Δ will be used below. Notice that b_n^0 is independent of D. Using Eq. (18), we obtain

$$\lambda_0^0 = 0.011\,37, \quad \lambda_0^1 = 0.007\,134,$$

$$\lambda_0^2 = 0.003\,008, \quad \lambda_1^0 \approx 1.85 \times 10^{-5}.$$

We see that λ_1^0 is two or three orders of magnitude smaller that λ_0^k, and the other λ_n^k's with $n \geqslant 1$ are even smaller. From Eq. (7) they decrease exponentially with increasing n. These values show that for most purposes we can disregard the contributions to the dynamics from deflections with $n > 0$: the measure of the set of orbits that make multiple turns around a black hole is negligible. This approximation will be used extensively in the next section.

Equations (16)–(18) are not exact, because the derivative $\Delta'(b)$ varies in the intervals Δb_n^k. To estimate the error, we use the fact that the Δb_n^k are small. The error $\delta\lambda_n^k$ in λ_n^k is then to first order

$$\delta\lambda_n^0 = \frac{\Delta b_n^0}{D} \frac{\Delta''(b_n^0)}{[\Delta'(b_n^0)]^2}, \qquad \delta\lambda_n^{1,2} = \frac{\Delta b_n^{1,2}}{L} \frac{\Delta''(b_n^{1,2})}{[\Delta'(b_n^{1,2})]^2}.$$

Using $\Delta b_n^k = \Delta b \lambda_n^k$, we get the fractional error $\delta\lambda_n^k / \lambda_n^k$,

$$\frac{\delta\lambda_n^0}{\lambda_n^0} = \frac{\Delta b}{D} \frac{\Delta''(b_n^0)}{[\Delta'(b_n^0)]^2}, \qquad \frac{\delta\lambda_n^{1,2}}{\lambda_n^{1,2}} = \frac{\Delta b}{L} \frac{\Delta''(b_n^{1,2})}{[\Delta'(b_n^{1,2})]^2}. \qquad (20)$$

The terms $\Delta''(b_n^k)/(\Delta'(b_n^k))^2$ are of the order of 1, and the terms $\Delta b/D$ and $\Delta b/L$ are much smaller than 1. Thus, the fractional errors in the values λ_n^k given by the approximate formula (18) are very small, of about 0.01 for $D = 15M$. In the limit of large D, we have $L \approx D$, and $\delta\lambda_n^k / \lambda_n^k \sim 1/D$: the fractional error is inversely proportional to the separation D, and the approximation (18) gets better and better as D increases.

IV. THE LIMIT $D \to \infty$

We now take the limit $D \gg 2b_{esc}$. From Eqs. (15) and (14), we have that in this limit $\alpha \to 0$ and $L \to D$. Equations (16) and (18) then imply that $b_n^k \to b_n^0 \equiv b_n$ and $\Delta b_n^k \to \Delta b_n^0 \equiv \Delta b_n$: the two intervals of surviving orbits of a given n come closer and closer as D increases, and their lengths become the same in this limit. Because of the approximate equality in the lengths, the magnification of each interval by $(\lambda_n)^{-1}$ gives approximately the same set of intervals. In other words, the fractal basin boundary is *self-similar* in this approximation.

The box-counting dimension of this self-similar set is given by the solution of the transcendental equation [10],

$$2 \sum_{n=0}^{\infty} (\lambda_n)^d = 1.$$

As we have seen in Sec. III λ_1 is many orders of magnitude smaller than λ_0. Therefore, it is a good approximation to neglect terms with $n > 0$ in the above expression, and d can then be explicitly written as

$$d = \frac{\ln 2}{\ln(\lambda_0)^{-1}}. \qquad (21)$$

From Eq. (18), we have $(\lambda_0)^{-1} = D|\Delta'(b_{esc})|$, and we get

$$d = \frac{\ln 2}{\ln D + \beta}, \qquad (22)$$

with $\beta = \ln|\Delta'(b_{esc})|$. For large D, the box-counting dimension decays logarithmically with the distance. If we substitute $D = 15M$, we get $d = 0.155$, in agreement with the numerical value of $d = 0.17 \pm 0.02$ discussed above, even though the limit $D \gg 2b_{esc}$ is only modestly satisfied at best.

V. THE CASE OF DIFFERENT MASSES

Now we consider the case of two black holes with different masses M_a and M_b. We restrict ourselves to the limit $D \gg 2b_{esc}^a, 2b_{esc}^b$, where b_{esc}^a and b_{esc}^b are the impact parameters corresponding to deflections of π of the two black holes. Because the two masses are different, the ranges Δb_a and Δb_b of impact parameters for surviving orbits are different, and therefore the allowed range of scattering angles depends on which black hole the orbit is heading to. This means that the "shrinking factors" λ_0^a and λ_0^b [given by Eq. (18)] depend on the black hole. This spoils the property of self-similarity, which is a feature of the equal-masses case in the limit $D \to \infty$. However, since the orbits are scattered alternately by the two black holes, the *square* of the scattering map defined by the system is self-similar, in the limit $D \to \infty$.

After two iterations, of each interval $[b_c, b_{esc}]$ there remains four subsets of surviving orbits, all with size of approximately $\lambda_0^a \lambda_0^b$ (we are not considering orbits with $n > 0$). Each of these subsets gives rise to four others after two further iterations, and so on. The box-counting dimension of the surviving set is given by [10] $4(\lambda_0^a \lambda_0^b)^d = 1$, that is

$$d = -\frac{\ln 4}{\ln(\lambda_0^a \lambda_0^b)}.$$

Substituting Eqs. (18) and (19) with M replaced by M_a and M_b, we obtain λ_0^a and λ_0^b, and we find

$$d = \frac{\ln 2}{\ln D + \beta + \ln \sqrt{\eta}}, \qquad (23)$$

where $\eta = M_a/M_b$, $\beta = \ln|\Delta'(b_{esc}^a)|$. The difference between Eqs. (23) and (22) is the constant term $\ln \sqrt{\eta}$ in the denominator of d. If $M_a = M_b$, then $\eta = 1$ and Eq. (23) is equal to Eq. (22), as of course it should. In the limit $D \to \infty$, d also decays logarithmically with distance in this case, as in the case of equal masses.

VI. CONCLUSIONS

In this paper we have studied the chaotic behavior of light rays orbiting a system of two nonrotating fixed black holes. We have assumed that the black holes are sufficiently far away from each other, so that we could consider the motion of the light rays to be the result of the action of each black hole separately. Since the equations of motion of a light ray in the space-time of an isolated black hole can be solved analytically, using this approximation we reduce the motion of the massless test particle to a two-dimensional map. Numerical integration of this map showed the existence of a fractal basin boundary, with an associated fractional box-counting dimension. In the limit of a large separation distance D between the two black holes, we have been able to obtain an analytical expression to the asymptotic value of the box-counting dimension d. We found that $d \sim (\ln D)^{-1}$ for large D; this result also holds for different black hole masses.

ACKNOWLEDGMENTS

[1] P.S. Letelier and S.R. Oliveira, Phys. Lett. A **238**, 101 (1998); D. Kramer, H. Stephani, M. MacCallum, and E. Herlt, *Exact Solutions of Einstein's Field Equations* (Cambridge University Press, Cambridge, 1980).

[2] G. Contopoulos, Proc. R. Soc. London, Ser. A **431**, 183 (1990).

[3] C.P. Dettmann, N.E. Frankel, and N.J. Cornish, Phys. Rev. D **50**, R618 (1994).

[4] S. Chandrasekhar, *The Mathematical Theory of Black Holes* (Oxford University Press, Oxford, 1992)

[5] I. D. Novikov and V. P. Frolov, *Physics of Black Holes* (Kluwer Academic Publishers, Dordrecht, 1988).

[6] G. Troll, Physica D **50**, 276 (1991).

[7] Y.-C. Lai and C. Grebogi, Phys. Rev. E **49**, 3761 (1994).

[8] L. D. Landau and E. M. Lifshitz, *The Classical Theory of Fields* (Pergamon Press, New York, 1975).

[9] W. H. Press, S. A. Teukolsky, W. T. Vetterling, and B. P. Flannery, *Numerical Recipes in C* (Cambridge University Press, Cambridge, MA, 1992).

[10] E. Ott, *Chaos in Dynamical Systems* (Cambridge University Press, Cambridge, 1993).

[11] E. T. Whittaker, *A Treatise on the Analytical Dynamics of Particles and Rigid Bodies* (Cambridge University Press, Cambridge, 1970).